INTERNATIONAL ATOMIC ENERGY AGENCY
UNITED NATIONS EDUCATIONAL, SCIENTIFIC AND CULTURAL ORGANIZATION

INTERNATIONAL CENTRE FOR THEORETICAL PHYSICS
34100 TRIESTE (ITALY) - P.O.B. 586 - MIRAMARE - STRADA COSTIERA 11 - TELEPHONE: 2240-1
CABLE: CENTRATOM - TELEX 460392-I

SMR/291 - 6

SPRING COLLEGE IN CONDENSED MATTER
ON
"THE INTERACTION OF ATOMS & MOLECULES WITH SOLID SURFACES"
(25 April - 17 June 1988)

CHEMICAL BONDS OUTSIDE SOLID SURFACES
(Lecture II)

N.H. MARCH
Theoretical Chemistry Department
University of Oxford
5 South Parks Road
Oxford OX1 3TG
UK

1.3.3 Hydrogenchemisorbed on Pt surface

Flores et al$^{(15)}$ considered the indirect lateral interaction (1.3.11) to attempt to interpret some experimental findings for H on Pt(111). Using such a pair potential description of lateral H–H interactions, these workers were able to interpret experimental information on surface stoichiometries and heat of adsorption and desorption. To apply the above result (1.3.11), one wished to establish that the H atoms occupy sites which enable H to lie in a region of high electron density. Flores et al cited such evidence as coming from (a) magnetic resonance measurements, (b) infra-red data and (c) neutron inelastic scattering. Elaborating (a) to illustrate the point, the magnetic resonance data show a state of adsorbed H with a large chemical shift in the opposite direction to the Knight shift. This can be interpreted as due to a proton lying in the region of high d–electron density from the metal atoms.

Using eqn (1.3.11) for $\Delta E(R)$, Flores et al reached the following conclusions:

(i) One can derive only one surface structure consistent both with the requirement that the minimum value of the pair potential must be associated with all possible near–neighbour distances and the Pt/H ratios found for the (111) plane of Pt.

(ii) The existence of 2 surface states of different bonding energies is required by the potential, which however are structurally and energetically equivalent at complete coverage of both sites. [This is in agreement with the convergence of the thermal desorption energies noted by Christmann et al$^{(16)}$].

(iii) The structure of the first H sites; those adsorbed on the clean surface; is consistent with the LEED studies of Weinberg and Merrill$^{(17)}$.

A fuller discussion of the work of Flores et al$^{(14)}$ can be found in the review by Burch$^{(18)}$ see also March$^{(19)}$. The work lends strong support to the importance of the asymptotic lateral interactions (1.3.11).

1.3.4 Lateral interaction between two CO molecules chemisorbed on Pt

Joyce et al(20) have considered the same type of lateral interaction (1.3.11) in attempting to interpret thermal desorption measurements as a function of coverage for CO chemisorbed on Pt.

Specially, these workers set up a model based on the molecular $2\pi^*$ and 5σ levels lying within the metal bands(cf Fig. 1.3.1.); the former above the Fermi level and the latter well below. Broadening of the former into a virtual bound state which can overlap the Fermi level can lead to a situation in which it is demonstrated that one can get strong indirect interactions between CO molecules. The amplitude β and phase ϕ of the long-range oscillatory form $\beta\cos(2k_fR+\phi)/R^5$ discussed in detail above can thereby be estimated. Table 1.3.1 shows the values of ϕ and β for an assumed coupling strength V between admolecule and substrate. ϕ is seen to be large, testifying to strong scattering of metal electrons by the adsorbate. We shall return below to briefly discuss the amplitudes β recorded also for various plausible values of the coupling strength in Table 1.3.1.

The results of the above model have been compared by Joyce et al(20) with an analysis they made of thermal desorption as a function of coverage for CO on Pt. Immediately the strong scattering situation predicted by the above model is revealed, with a phase shift between $\pi/4$ and $\pi/2$ and a large amplitude β. To press the comparison with the model, a least squares fit made of the experimental decrease in the desorption energy by Joyce et al gave $\phi = 0{\cdot}95$, and $\beta = 1{\cdot}0 \times 10^7$ J mol^{-1} Å^5. Though the agreement for β is only semiquantitative , it seems remarkable that such a simple model gives the gist of the experimental findings.

1.4 Molecular versus dissociative adsorption on transition metal surfaces

We conclude with a discussion of trends in chemisorption, of a more general kind. Specifically, one wants to analyze the behaviour of small molecules like CO,N_2, NH_3, etc. on transition metal surfaces. A pattern emerges from an analysis of data on various adsorbate-substrate systems. For a given molecule, metals to the left of a line dividing the Periodic Table dissociate the molecule, while those to the right adsorb it with its chemical bond(s) intact.

Below, we shall present a chemical approach which is based on Pauling's treatment(21) of bond energies in free molecules. This treatment was adapted by Eley(22) and other workers to the chemisorbed state. Specifically, Eley obtained estimates of adsorption heats by employing Pauling's equation in calculating the metal atom–adsorbate atom bond energy denoted by E(M–A). This quantity is thereby expressed in the form

$$E(M\text{–}A) = \tfrac{1}{2}\left[E(M\text{–}M) + E(A\text{–}A)\right] + (x_m - x_A)^2 \tag{1.4.1}$$

where E(M–M) and E(A–A) are the single bond energies of metal and diatomic molecule, respectively, while x_m and x_A are the corresponding atomic electronegativities. Eqn (1.4.1) is written in electron volts.

It is true that eqn (1.4.1) has limitations as a route to the calculation of accurate bond energies, because of its sensitivity to the electronegativity difference. Nevertheless, the work of Flores et al(23), which will be utilized in the ensuing discussion, demonstrates that eqn (1.4.1) is adequate for the purpose of interpreting the general pattern of dissociative versus molecular adsorption, provided a term due to metal–metal bond breaking is added. To the writer's knowledge, a fully quantitative basis for such a term from wave mechanics has not, so far, been given. Therefore

Flores et al$^{(23)}$ use as input data into this term representing the breaking of metal bonds, a measure of valence as obtained from wave mechanical band-structure calculations. With this addition, Flores et al demonstrate that eqn (1.4.1) is indeed adequate to expose a pattern of behaviour for the chemisorption of a given adsorbate on a variety of transition metals.

1.4.1 Reactivity of metal towards molecular adsorbate

If geometric factors are ignored, as well as metal bond breaking for the time being, the reactivity of a metal towards a molecular adsorbate is determined by:

(1) The dissociation energy of the molecule in free space.

(2) The strength of the bonds formed between its constituent atoms and the metal.

(3) Molecular chemisorption energies.

For most of the systems of interest here, (3) is considerably smaller than (1) or (2), and provided one is focussing on the pattern of behaviour rather than fully quantitative work, Flores et al$^{(23)}$ argue that it may be neglected. Then, for instance in the case of a diatomic molecule, one must clearly compare the energies involved in (1) and (2) above. To study (2), it is important to consider next a tractable, if somewhat over-simplified, way in which bonding in transition metals is to be handled.

1.4.2. Bonding and valence in transition metals

A useful description of bonding in transition metals can be given in terms of overlapping hybrids on neighbouring atoms. These hybrids are formed from the s, p and d orbitals in such a manner that they are directed towards nearest and next-nearest neighbours in the crystal.

(a) Resonating bonds

Consider as a specific example the case of a face-centred-cubic (fcc) transition metal for which the 12 nearest neighbours make the major contribution to the bonding. In principle then the number of hybrids is six or less. This calls for a description of the ground electronic state in terms of a number of resonating states, so that, on average, there is a hybrid pointing towards each of the 12 near-neighbour atoms.

Of course, it is a direct consequence of this picture that only a fraction of an electron can be shared in each bond between atoms: this is expressed in Pauling's concept of metallic valence$^{(21)}$. One then wishes to associate the fractional occupation of the hybrids with some average valence, defined as the total number of electrons used for bonding to the neighbouring atoms.

Though the above discussion referred specifically to a fcc crystal, in fact for a hexagonal closed packed (hcp) metal the local coordination number is also 12 while in a body-centred-cubic (bcc) structure there are eight near neighbours and six next-near neighbours. Thus, even for the bcc structure, the assumption of 12 hybrids around each atom should provide a useful average description.

(b) Calculation of average valence

Returning to the question of the average valence, it is important to chose this to be consistent with the available knowledge on the electronic charge distribution in the energy bands of transition metals. For, in spite of the strong electron-electron correlation that Pauling's ideas correctly incorporate, it is known from density functional theory that correlation can be subsumed into a one-body potential in calculating, in principle exactly, the electronic charge density in the ground state from energy band theory.

Therefore Flores et al$^{(23)}$ made use of the augmented plane wave (APW) calculations of Moruzzi et al$^{(24)}$ for the energy bands of transition metals, to obtain the number of interstitial electrons per atom in the crystal. This number they defined from the APW calculation as the number of electrons outside the muffin–tin sphere. Their proposal was to correlate this quantity with the number of bonding electrons, the reason being that the localized electrons are not shared in bonds and contribute only to the charge in the immediate vicinity of one atom.

Then it was natural to assume the average valence proportional to the number of interstitial electrons. By choosing the proportionality constant to yield a valence of 1 for Na and 3 for $A\ell$ with bcc and fcc structures respectively, the average valences obtained were as recorded in Table 1.4.1.

At the time of writing, we are not aware of similar quantitative calculations for the number of interstitial electrons in the third transition series. Therefore, in order to extend their analysis to these elements, Flores et al(23) assigned the valences of the second–row elements to them since, in general, properties of the third transition series resemble more closely the second series than the first. It is clear, however, that one can expect, because of this over–simplified treatment of valence in the third series, one ought, at most, only to consider the general trends in this case.

It is of some interest to comment briefly on the average valence recorded in Table 1.4.1 in relation to Pauling's maximum valence. Pauling assigned a valence of 6 to the elements Cr to Ni and 5½ to Cu : these are 2–3 units larger than the proposals of Flores et al(23). It had been suggested already by Hume–Rothery et al(25) that the metallic valence is less for the elements of the first long periods than it is in the later periods. On the basis of the physical properties of the elements, these workers(25) suggest that V and Cr do not involve more than 4 bonding electrons per atom and that Mn has a relatively low valence of about two, followed by a rise in passing to Fe. A decrease in valence through group VIII is more evident in the second and third periods. Flores et al drew attention to the fact that their proposed scheme is supported by the relative importance of the valences exhibited in the chemistry of the transition elements.

Table 1.4.1 giving the average valence can now be employed to estimate metal–metal bond energies by dividing twice the cohesive energy by the average valence. These values are recorded in Table 1.4.2. These, it should be added, differ substantially from those given in the much earlier work of Eley et al(26), who obtained metal–metal bond energies by dividing twice the heat of sublimation by the number of nearest neighbours.

1.4.3 Admolecule bonding to a metal surface

Given the concept of average valence as above, and the estimated metal–metal bond energies thereby obtained, as in Table 1.4.2, Flores et al(22) discussed the bonding at the surface along the following lines.

They regarded each surface atom as having a number of dangling bonds, determined by the crystal structure and the particular crystal face, while the number of electrons occupying these bonds is governed by the average valence, v say, of Table 1.4.1. For instance, each surface atom on the (111) face of a fcc crystal has three dangling bonds with $v/12$ electrons in each. Due to the similarities of local coordination in fcc, hcp and bcc crystals referred to above, Flores et al assumed that this is true for a dangling bond on any face. This implies that in order to form one bond with the adsorbate, other $(1-v/12)$ metal electrons are required for sharing. More generally, a number of metal bonds, n say, depending on the particular crystal face and on the adsorbate, will have to be broken in order to saturate the metal–adatom bond. Thus eqn (1.4.1) can be modified to read

$$E(M\text{–}A) = \tfrac{1}{2}\,[E(M\text{–}M) + E(A\text{–}A)] + (x_m - x_A)^2 - nE(M\text{–}M), \qquad (1.4.2)$$

which the starting point for the calculations of Flores et al$^{(23)}$.

Flores et al consider on the basis of eqn (1.4.2) the energetics of N_2, O_2, CO and NO chemisorption on transition metals. Without appeal to specific crystal structures, for the reasons given above, Flores et al assume that of oxygen and nitrogen, every hybridized atomic orbital can form a bond with the metal surface. For carbon, in contrast, it is not clear how many bonds can be formed with the surface : since the interaction with the surface influences the valence of carbon.

As one example, merely to illustrate trends, Flores et al write, on the basis of the arguments given above, that the energy of chemisorption of one nitrogen atom is:

$$E(M\text{–}N) = 3\Big\{\tfrac{1}{2}\Big[E(M\text{–}M) + E(N\text{–}N)\Big] + (x_m - x_N)^2 - (1 - v/12)E(M\text{–}M) \qquad (1.4.3)$$

In eqn (1.4.3) the factor 3 accounts for the number of bonds formed between nitrogen and the metal. Clearly, eqn (1.4.3) is sensitive to the difference $(x_M - x_N)$, as considered in the calculations now to be briefly summarized.

Eqn (1.4.3) must only be applied when E(M–N) is greater than that energy obtained by assuming a fractional bond order given by v and no breaking of the metal bonds. Anticipating the results in Table 1.4.3 below, it is to be noted that this latter energy is in fact higher for Pt and Ir, and in these two cases it is then the appropriate values that are recorded. For these two metal surfaces, instead of E(M–N) given by eqn (1.4.3), the bond energy $\{\tfrac{1}{2}[E(M\text{–}N) + E(N\text{–}N)] + (x_m - x_N)^2]\}$ must be multiplied by v/12, the fractional bond order referred to above.

The metal–nitrogen bond energies obtained from eqn (1.4.3) combined with data from Tables 1.4.1 and 1.4.2. are collected in Table 1.4.3. These should be compared with 4·8eV which is half the dissociation energy of N_2, in order to determine whether dissociation or molecular adsorption is likely to occur.

The solid line in Table 1.4.3 shows the experimental boundary according to Brodén et al$^{(27)}$. Agreement between theory and experiment seems satisfactory when one bears in mind the large errors originating from the theoretical estimates, due to the wide extremes of electronegativity quoted by Gordy and Thomas$^{(28)}$.

1.5 Summary and some future directions

Of course, as will be clear from this discussion, for fully quantitative results there is no substitute for fairly detailed computations on the specific system under discussion.

Thus, as Appendix 1.3 makes clear, the type of argument presented for physisorption in section 1.2 needs refinement to take account of the discrete nature of the solid substrate.

There is evidently scope for much further work on indirect lateral interactions mediated by the itinerant metal electrons, along lines laid down for CO–CO interactions in section 1.3.4. As stressed there, one probably needs to appeal to photoelectron spectroscopy to 'place' the molecular energy levels relative to the metal Fermi level. Given such an empirical level diagram, we expect the method outlined in section 1.3.4 to have wide applicability, even to substantially more complex molecules than considered here.

While conformational studies remain of considerable interest, it is obvious for the future that reaction rates of chemical reactions outside solid surfaces remains a challenging area for theoretical chemical physics. Can simple arguments and/or concepts be found which will allow an understanding of the way the lowering of activation barriers can come about in catalysed reactions. Can likewise concepts be isolated to permit deeper understanding of Sabatier's concept of activated complex? Of course, much computational study already is recorded in the literature related to the above. What seems needed is a synthesis of this and, more importantly, experiment, using arguments and concepts that combine collective

excitations possible for the solid surface and reactants in strong interaction with the above ideas of activation barrier lowering and intermediate complexes.

Table 1.3.1

Values of amplitude β and phase ϕ in lateral long–range oscillatory interaction between CO molecules on Pt as a function of coupling parameter V.

V(eV)	3·5	4·0	4·5	5·0
β(Jmol^{-1}Å^{5})	$0{\cdot}26\text{x}10^{7}$	$0{\cdot}41\text{x}10^{7}$	$0{\cdot}58\text{x}10^{7}$	$0{\cdot}79\text{x}10^{7}$
ϕ	0·75	0·98	1·19	1·39

Table 1.4.1

Average valences assigned to transition metals

(after Flores et al$^{(23)}$)

Ti	V	Cr	Mn	Fe	Co	Ni	Cu
3·4	3·3	3·4	3·5	3·5	3·2	2·9	2·6
Zr	Nb	Mo	Tc	Ru	Rh	Pd	Ag
4·0	4·0	4·2	4·3	4·1	3·6	3·1	2·7

Table 1.4.2

Metal-metal bond energies in electron volts*

Ti	V	Cr	Mn	Fe	Co	Ni	Cu
2·89	3·00	2·26	1·66	2·57	2·81	3·12	2·70
Zr	Nb	Mo	Tc	Ru	Rh	Pd	Ag
3·20	3·60	3·06	3·07	3·30	3·18	2·55	2·24
Hf	Ta	W	Re	Os	Ir	Pt	Au
(3·14)	(3·86)	(3·88)	(3·77)	(4·01)	(3·80)	(3·82)	(2·85)

*Numbers in parentheses were found using valences as for the second-row series.

Table 1.4.3

Energy of metal-nitrogen atom bond in electron volts (after Flores et al$^{(23)}$)

Cr^{D}	Mn^{D}	Fe^{D}	Co	Ni^{M}	Cu^{M}
7·0	8·3	5·8	5·2	3·8	4·2
Mo^{D}	Tc	Ru	Rh^{M}	Pd^{M}	Ag
6·2	–	4·1	3·4	3·1	5·0
W	Re	Os^{M}	Ir^{M}	Pt^{M}	Au^{M}
(5·2)	(4·3)	(3·5)	(3·5)	(2·6)	(2·5)

N.B. Estimated errors are given by Flores et al$^{(23)}$.

M denotes molecular adsorption while D refers to dissociation. Absence of labelling means no decisive conclusion.

(Values in parentheses indicate that the same valences were used in series 3 as in series 2).

Fig 1.3.1

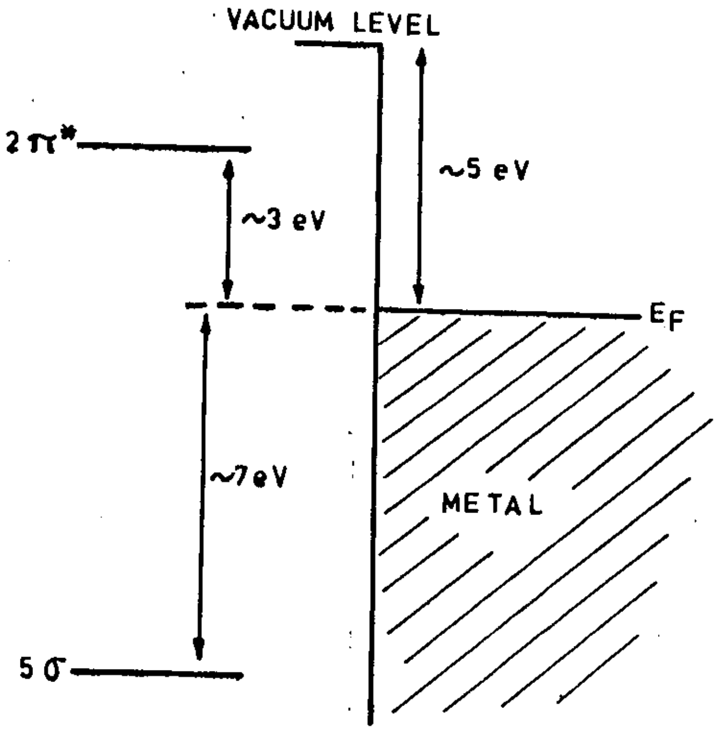

Shows $2\pi^*$ and 5σ levels of CO molecule adsorbed on Pt metal surface. E_F is the Fermi level.

Fig 1.1

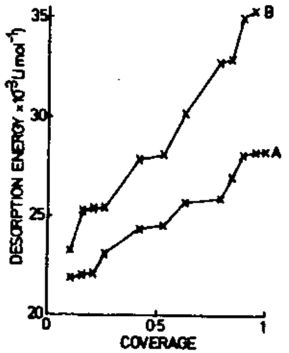

Variation of desorption energy with coverage.